Disulphide Crosslinked Star Block Copolypeptide Hydrogels: Influence of Block Sequence Order on Hydrogel Properties

Journal:	*Polymer Chemistry*
Manuscript ID	PY-ART-05-2018-000741.R1
Article Type:	Paper
Date Submitted by the Author:	22-Jun-2018
Complete List of Authors:	Murphy, Robert; Royal College of Surgeons in Ireland, Medicinal and Pharmaceutical Chemistry in het Panhuis, Marc; University of Wollongong, School of Chemistry Cryan, Sally-Ann; Royal College of Surgeons Ireland, School of Pharmacy Heise, Andreas; Royal College of Surgeons in Ireland, Medicinal and Pharmaceutical Chemistry; Dublin City University, School of Chemical Sciences

Polymer Chemistry

ARTICLE

Disulphide Crosslinked Star Block Copolypeptide Hydrogels: Influence of Block Sequence Order on Hydrogel Properties

Received 00th January 20xx,
Accepted 00th January 20xx

DOI: 10.1039/x0xx00000x

www.rsc.org/

Robert Murphy,[a] Marc in het Panhuis,[b] Sally-Ann Cryan,[c,d,e,f] and Andreas Heise*[a,f]

Reported are a series of 32- and 64-arm star shaped diblock copolypeptides containing opposite block sequences of oligo(cysteine) and poly(lysine) resulting in hydrogels comprising core and shell mediated disulfide crosslinking. Spontaneous gelation was observed within minutes of aqueous immersion, without any necessary pretreatment at concentrations as low as 0.05 wt%. The secondary structure underwent a change in agreement with the gel-sol transition as evidenced by a combination of FT-IR and CD spectroscopy. Changing the sequence on the 32-arm from core crosslinking to shell crosslinking had a significant effect on hydrogel storage modulus as it changed from 820 Pa to 4530 Pa. Notably, changing the polypeptide block sequence order had a direct effect on mechanical properties (including self-recovery behaviour). While the core crosslinked hydrogel underwent shear induced recovery almost instantaneously after passing through a standard syringe needle, the shell crosslinked hydrogel expelled water when subject to the same shear. The responsiveness of the molecular system to redox stimuli provides further desirable attributes that could allow for controlled, targeted delivery of therapeutic payloads.

Introduction

Polymeric hydrogels, which are a class of gelating materials comprised of a three-dimensional (3-D) crosslinked network, have received considerable attention in recent times for their applicability in biomedical science. Of particular interest is their use as drug/gene delivery systems, tissue engineering scaffolds or bio-devices such as sensors.[1] Hydrogels have been prepared from a variety of biocompatible natural and synthetic polymers including polysaccharides and vinyl polymers.[2,3] In synthetic polymers, pre- and post-polymerisation modifications can be readily achieved allowing for inclusion of functional groups that can facilitate gelation and the hydrogels produced can exhibit self-recovering, self-healing or shear thinning behaviour.[4-6]

Polypeptides represent excellent candidates for hydrogelating materials as they possess a number of desirable properties. They bear a variety of different side chain functionalities, can orientate into ordered conformations stabilising their structures and can also hydrolyse in the presence of enzymes similar to protein degradation.[7,8] Hydrogel networks prepared from biomimetic polypeptides also display similar physicochemical properties to those compositions found in the extracellular matrix (ECM).[9] Ordered conformation of parallel peptide strands results in self-assembly through secondary interactions such as α-helical or β-sheet assemblies,[10,11] akin to that of native proteins.[12] As a result, much recent literature surrounds the use of synthetic polypeptides as hydrogelators due to their likeness to biomolecules.[13-15]

The facile nature of the N-carboxyanhydride (NCA) ring opening polymerisation (ROP) for polypeptide production as well as the use of orthogonal chemistries has helped to develop versatile fabrication

[a] Department of Chemistry, Royal College of Surgeons in Ireland, Dublin 2, Ireland. Email: andreasheise@rcsi.ie
[b] Soft Materials Group, School of Chemistry, and Australian Research Council Centre of Excellence for Electromaterials Science, University of Wollongong, Wollongong, NSW 2522, Australia.
[c] Drug Delivery & Advanced Materials Team, School of Pharmacy, RCSI, Dublin, Ireland.
[d] Tissue Engineering Research Group, Department of Anatomy, RCSI, Dublin, Ireland.
[e] Trinity Centre for Bioengineering, Trinity College Dublin (TCD), Dublin, Ireland.
[f] Centre for Research in Medical Devices (CURAM), RCSI, Dublin and National University of Ireland, Galway, Ireland.
Electronic Supplementary Information (ESI) available: GPC plots, SEM and Rheology data.

systems in order to design advanced structures.[16-19] The versatility of the synthesis allows for development of hybrid polypeptide hydrogel systems which can be tailor-made for biomedical applications.[20,21] The crosslinks necessary for network formation are induced by independent hydrophobic physical or chemical interactions linked to a water soluble domain.[22] Chain aggregation can occur through micellar or fibril assembly due to adjacent crosslinks arising from α-helical and β-sheet conformations, resulting in alternative self-assembly patterns.[23,24]

Hydrogels based on polypeptides can also undergo morphological adjustments in the form of sol-gel/gel-sol transitions or network shrinking. These transitions are a direct result of changes in pH,[25] temperature,[26,27] chemical environment[28,29] or light.[30,31] Among synthetic polypeptides with stimuli triggered assemblies, there is a great deal of interest in responsiveness via redox mechanisms due to the nature of the intracellular environment. The tripeptide, glutathione (GSH), is the most abundant non-protein based thiol present in the intracellular environment. Its main role within the cell is to regulate the redox process through the generation of a highly reducing medium for biomolecules, thereby preventing molecular oxidation.[32] Particularly interesting sites of action for GSH are residues consisting of disulphide linkages, which readily undergo cleavage in its presence.[33] This has generated significant materials research interest due to the straightforward nature of disulphide formation in thiol containing macromolecules.[34] Thus, many research groups have explored the use of these covalent bonds as active groups in their polymeric architecture for responsiveness.[35,36] A number of researchers have described the inclusion of oligo or poly-L-cysteine sequences in their synthetic polypeptides due to the spontaneous thiol-disulphide conversion.[37-39] The preparation of polypeptide based hydrogels have also been explored through the integration of disulphide forming residues.[40,41]

There are very few studies on the design and development of hydrogel systems based on star shaped polypeptides.[42,43] We have recently reported the design of a series of hydrogelating scaffolds from star block copolypeptides tethered to an 8-arm dendritic core.[44] The degree of polymerisation was identical for both the hydrophilic inner blocks (poly-L-lysine) and the hydrophobic outer blocks (poly-L-tyrosine, poly-L-phenylalanine, poly-L-valine). Contrasting chemical character of the side chain functionalities (phenol, phenyl, isopropyl) allowed for modulation of the rheological and gelation properties, which proved to be sensitive to the composition of the shell sequence. All hydrogels exhibited shear thinning properties and could be injected with acceptable force with gelation concentrations ranging from 1.25 to 2.0 wt% and storage moduli from 180 to 2210 Pa. Superior mechanical properties are associated with hydrogels prepared from these star shaped architectures in comparison to linear polypeptides. Using the same principles, we have also used supramolecular star diblock copolypeptide hydrogels as bio-inspired inks in the development of constructs via 3D extrusion printing.[45] Based on short glutamic acid and valine chains tethered to a 32-arm dendrimer with UV-curable functionalities, the 3D hydrogel scaffolds produced could load molecular cargo, were hydrolytically degradable and displayed no cytotoxicity when biocompatibility was assessed using 3T3 fibroblasts. Moreover, both non-gelating and gelating stars display a more efficient loading capacity and improved delivery properties compared to conventional linear polypeptides.[46-48]

Inspired by previous reports on the influence of block sequence in linear block copolypeptides on their properties,[49,50] we present the synthesis of a series of star shaped diblock copolypeptide hydrogels possessing differing properties based on covalent interactions between disulphide bridges within the core and the shell of the star architecture. Changing sequence order from core disulphide to shell disulphide results in a transition from shear thickening to shear-thinning/self-recovering hydrogels. The materials were readily prepared via the sequential ring opening polymerisation (ROP) of N-carboxyanhydride (NCA) monomers benzyl-L-cysteine (BLC) and ε-carbobenzyloxy-L-lysine (ZLL) with two highly branched poly propylene imine (PPI) dendritic initiators. The characteristics, including the conformational and mechanical character, of each polypeptide hydrogel were studied. Results and evaluation of the secondary structure, rheological properties and reduction triggered drug release via dithiothreitol (DTT) are all outlined in order to demonstrate their suitability as biomedical hydrogels.

Experimental

Materials

All chemicals were obtained from Sigma-Aldrich unless otherwise stated. ε-Carbobenzyloxy-L-lysine and benzyl-L-cysteine were purchased from Novachem. Generation 4 (G4) and generation 5 (G5) poly-propylene imine (PPI) dendrimers were obtained from SyMO-Chem BV. The NCAs of ε-carbobenzyloxy-L-lysine and benzyl-L-cysteine were synthesised following literature procedures.[51]

Methods

^{1}H-NMR spectra were recorded on a Bruker Advance 400 (400 MHz) spectrometer at room temperature (21 °C) with trifluoroacetic acid-d (TFA-d) as a solvent. Attenuated total reflection (ATR) FT-IR was recorded using a Thermo Scientific iS10 spectrometer in the region of 4000–400 cm^{-1}. A background measurement was initially performed before analysing the sample. Sixteen scans were completed using a resolution of 2 cm^{-1}. Circular dichroism spectra were acquired using a Jasco J-810 spectropolarimeter in the UV region (180 to 280 nm). The polypeptides were analysed at a concentration of 0.01 mg mL^{-1} (deionised water) in a quartz cell with a path length of 0.1 cm. Baseline correction was achieved by using deionised water as a reference before sample measurement. The scans were recorded at a speed of 20 nm min^{-1} with a data pitch of 0.1 nm. The sensitivity was set to 10 mdeg with a response time of 3 sec and a bandwidth of 1 nm. The mean residue ellipticity was calculated using the following equation:

(1) $$[\theta]MRW = ([\theta] \times MRW)/(10 \times l \times c)$$

with experimentally determined (Θ) in mdeg, mean residue weight (*MRW*) in g mol^{-1}, path length (*l*) in cm and sample concentration (*c*) in mg mL^{-1}. The molecular weight and molecular weight distributions (dispersity, $Đ = M_w/M_n$) were determined by Size Exclusion Chromatography (SEC). Monodisperse polystyrene standards were used to generate a standard calibration curve. SEC measurements were carried out on a Waters 515 equipped with a Wyatt DAWN HELEOS-II (laser 658.0 nm) laser light scattering detector and a Wyatt Optilab rEX detector. The eluent was THF with a flow rate of 1 mL min^{-1}. The column temperature was set to 40 °C and the refractive index detector at 40 °C.

Imaging and Mechanical Analysis

Scanning Electron Microscopy (SEM) was carried out on a JEOL JSM 6490LV SEM with an excitation voltage of 15 kV. The sample was gelled at 3.0 wt% and then frozen in small spherical moulds prior to imaging. Rheological measurements were performed on an Anton Paar Physica MCR 301 digital rheometer. All experiments were conducted at room temperature (21 °C) using a conical plate consisting of a 50 mm diameter geometry and a 1° cone angle with a gap length of 0.097 mm. The use of a temperature-controlled hood was employed to prevent evaporation of water from the hydrogels. The weight swelling ratio (Q) of the hydrogel samples was determined using the following equation:

(2) $$Q = (M_S - M_R) / M_R$$

where M_R is the hydrogel mass in dry state and M_S is the hydrogel mass in the swollen state.

Drug Release

DOX.HCl was prepared as a 1 mg mL^{-1} solution in deionised water. The hydrogel/drug depot was prepared resuspending the lyophilised polypeptides using the DOX.HCl solution (1 mg mL^{-1}) at a polypeptide concentration of 3.0 wt%. The samples were stirred overnight and allowed to sit for two days before analysis. The drug loaded hydrogel samples were dialysed (12-14kDa MWCO) against 50 mL of PBS (pH 7.5, room temperature), with the addition of 10 mM DTT to the media for the reduction assay, to determine drug release over time. Aliquots of the dialysate were assayed for DOX.HCl content at specific time intervals using a UV/vis spectrometer at 490 nm. Quantification was determined using a calibration curve and samples were then returned to the media.

Preparation of 64-arm oligo-L-cysteine-*b*-poly-L-lysine (64-OLC$_5$-b-PLL$_{40}$)

The NCA of benzyl-L-cysteine (176.36 mg, 7.43×10^{-1} mmol) was dissolved in anhydrous $CHCl_3$ (6 mL) under a N_2 atmosphere. The flask was placed in a termostatically controlled water bath containing 5M NaCl at 0°C. The 64-arm G5 PPI dendrimer (16.65 mg, 2.32×10^{-3} mmol) was solubilised in 4 mL of dry $CHCl_3$, and quickly added to the Schlenk flask. The flask was evacuated under vacuum to remove the CO_2 generated and stirring was allowed for 20 hours at 0°C. FT-IR was used to confirm total consumption of the BLC NCA monomer. The NCA of ε-carbobenzyloxy-L-lysine (1.82 g, 5.95 mmol) was dissolved in 15 mL anhydrous $CHCl_3$ and charged to the Schlenk flask. The solution was allowed to stir at 0°C until full conversion of the ZLL NCA monomer was confirmed by FT-IR. The polymer was precipitated into excess diethyl ether and dried under vacuum in a dessicator to give the 64-PLC$_5$-b-PLL$_{40}$ star polymer (yield 82 %). Subsequently, the dried polymer (1.1 g) was dissolved in 15 mL trifluoroacetic acid and allowed to stir until fully dissolved. Then, 6 mL of HBr (33% wt. in acetic acid) was added drop wise to the solution in a six-fold molar excess with respect to ε-carbobenzyloxy-L-lysine and benzyl-L-cysteine protecting groups and stirring continued for 16 hours. The polymer was precipitated twice into diethyl ether (40 mL) and

centrifuged. The TFA/HBr/diethyl ether waste was decanted and the precipitate was washed once more with diethyl ether. The material was dried under vacuum and then subsequently dissolved in deionised water. Dialysis was performed against deionised water for 4 days using a 12-14 kDa MWCO membrane, with frequent water replacement. The polymer was then lyophilised (yield 60%). The other diblock copolypeptides were prepared accordingly replacing the 64-arm G5 PPI dendrimer initiator with the 32-arm G4 PPI dendrimer while proprgylamine was used for the linear copolymer. For the homopolypeptide ZLL NCA was used.

Results and Discussion

Preparation of star copolypeptides

The 32-arm star diblock copolypeptides with alternating sequences of oligo(benzyl-L-cysteine)-*b*-poly(Z-L-lysine) were synthesised via the ROP of corresponding NCA amino acid monomers using a G4 poly(propylene imine) (PPI) dendrimer initiator. Alternating between the amino acid monomer addition allowed for core tethered sequences using BLC NCA followed by peripheral polymerisation of ZLL NCA or *vice versa*, maintaining a ratio of 5 cysteine to 40 lysine per arm (Fig. 1). FT-IR spectroscopy confirmed the consumption of the first NCA monomer, after which the second monomer was added, and chain extended through the terminal amine. ^{1}H-NMR was used to confirm the successful growth of the polypeptide chains from the primary amines on the dendrimer and from the terminal amine first block (Fig. S2). An additional 64-arm star copolypeptide with an inner oligo(benzyl-L-cysteine) and shell poly(Z-L-lysine) sequence was synthesised in order to investigate the correlation between degree of branching and material properties. The architecture was composed of the same arm length but double the number of arms relative to the 32-arm dendritic initiator. The relative molecular weights were analysed via size exclusion chromatography (Fig. S1, Table S1), showing a trace shift in agreement with target degree of polymerisation (DP). In order to reveal the pendant functionalities of the polypeptides (amine and thiol), cleavage of the protecting groups was achieved with TFA and HBr (33 %) in acetic acid. The polymers are denoted as 32-OLC_5-b-PLL_{40}, and 32-PLL_{40}-b-OLC_5, respectively.

Each of the star diblock copolypeptides formed hydrogels at low material concentration. No pretreatment was necessary as they spontaneously gelled in aqueous media (Fig. 1). The critical gelation concentration (CGC) was determined using the inversion vial method (Table 1). It was considered a gel since no flow was evident within five minutes of inversion. Interestingly, the network of hydrogel samples formed at very low concentrations, in particular for the 32-arm shell crosslinked star copolypeptide, which remained a stable gel at 0.05 wt%. The CGC increased significantly to 0.5 wt% for the 32-arm core crosslinked hydrogel, with a slightly lower polymer concentration sufficient for gelation of its 64-arm analogue (0.3 wt%). Switching the peptide sequence pattern has a definitive effect on the gelation, with a magnitude of ten difference observed for alternative 32-arm hydrogels. A linear copolymer with a DP ten times that of the equivalent arms of the stars was synthesised (1-$PBLC_{50}$-b-$PZLL_{400}$) and did form a hydrogel but at notably higher concentrations than the stars.

Table 1. Properties of hydrogels at 21 °C. CGC and G' are the critical gel concentration (determined using inversion method) and storage modulus in the linear visco-elastic region. Q is calculated using equation 2.

polymer	CGC (wt%)	G' (Pa)	weight swelling ratio (Q)
32-PLL_{40}-b-OLC_5	0.05	4530 [a]	87.4 [a]
32-OLC_5-b-PLL_{40}	0.5	820 [a]	63.1 [a]
64-OLC_5-b-PLL_{40}	0.3	1230 [a]	67.4 [a]
1-$PBLC_{50}$-b-$PZLL_{400}$	4.5	430 [b]	45.6 [b]

[a] Analysed at 3.0 wt%. [b] Analysed at 6.5 wt%.

Visual inspection of core and shell disulphide hydrogel networks under SEM, which were obtained from a hydrated gel sample that was frozen prior to imaging, show porous interconnected networks (Fig. S3). Irregular assemblies can be observed denoting parallel structures with many interwoven fibres observed.

Polymer Chemistry

ARTICLE

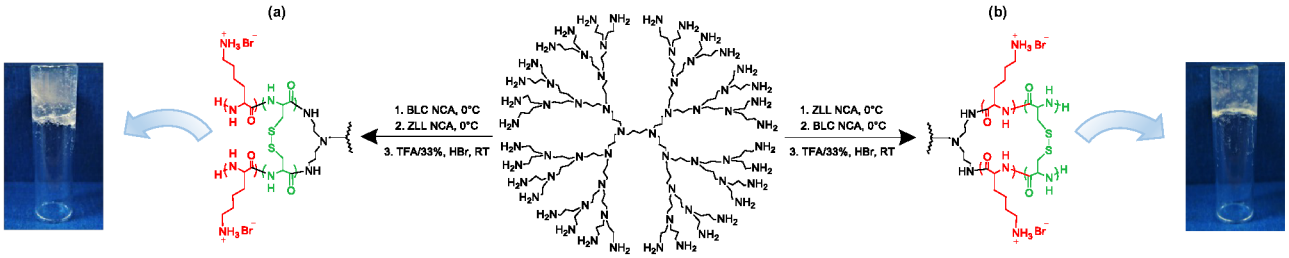

Fig. 1 (a) Synthetic route of 32-OLC_5-b-PLL_{40} with an image of its subsequent aqueous gelation. (b) Synthetic route of 32-PLL_{40}-b-OLC_5 with an image of its subsequent aqueous gelation. *two neighbouring arms denoted in each of the final chemical structures.

The alignment of such fibres depicts accumulation of aggregates possibly representing micellar assemblies.[43,52,53] It is anticipated that the core crosslinked hydrogel network is governed by the conformation stemming from disulphide linkages primarily formed through intramolecular crosslinking junctions with thiol residues on the same star or intramolecular folding on the same arm. Intermolecular crosslinking of adjacent thiol in the core stars would be difficult considering their location within the star structure, although this would be more viable for the shell crosslinked hydrogel network with pendant thiols on the periphery of the architecture. In order to investigate the orientation of disulphide from the short chain oligo(L-cysteine) sequences close to the core and on the periphery, FT-IR and CD spectroscopy was used.

Conformational analysis

FT-IR analysis of the polypeptides in the solid and gelled state uncovered the conformational changes resulting from the polypeptide chain folding in the amide I and II regions from 1500-1700 cm^{-1} (Fig. 2). Of the star polypeptides made with core and shell disulfide linkages, there are significant deviations in the FT-IR pattern when compared to the star homopolypeptide 64-PLL_{40} (Fig. S4). For the each of the shell and core disulfide crosslinked polypeptide materials, there is a nominal shift in the bands from alternative conformations arising from both gelled and solid states. For lyophilised 32-OLC_5-b-PLL_{40}, the bands at 1670 and 1629 cm^{-1} become significantly more pronounced after gelling in D_2O (Fig. 2a), with each of the bands representing characteristic β-turn and β-sheet conformations respectively.[54] The characteristic β-sheet band at 1633 cm^{-1} becomes apparent after swelling overlapping the random coil band at 1649 cm^{-1}. The increase of the β-turn band 1671 cm^{-1} could possibly signify the presence of multiple intramolecular disulphides arising from linkages of neighbouring cysteine residues from the core oligo-L-cysteine sequences.[55] The intramolecular crosslinking of cysteines on the same polypeptide arm sequence and on neighbouring arm sequences could influence the presence of β-motifs, which are well established in short hydrophobic peptide sequences.[56,57]

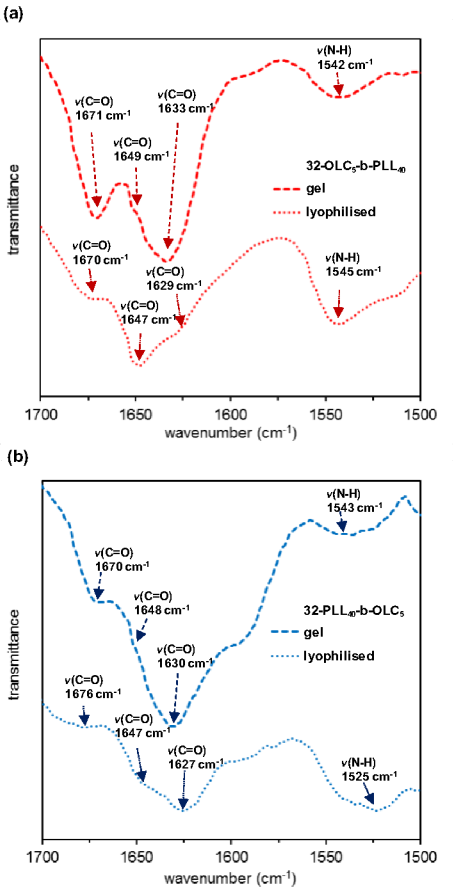

Fig. 2 FT-IR spectra of solid (dotted lines) and gelled (dashed lines) state core and shell disulphide crosslinked copolypeptides: (a) 32-OLC_5-b-PLL_{40}, (b) 32-PLL_{40}-b-OLC_5.

Comparatively for the gelled 32-PLL_{40}-b-OLC_5 material (Fig. 2b), the intensity of the characteristic β-turn band at 1670 cm^{-1} is modest considering the intensity of the β-sheet band at 1630 cm^{-1}, which could imply the presence of intermolecular disulphide formation between adjacent star copolypeptides with shell oligo-L-cysteine.[58,59] In addition to FT-IR, CD spectroscopy provides further insight into the conformation associated with polypeptide macromolecular architecture in solution. CD analysis was used in conjunction with FT-IR in order to correlate the spectroscopic results. In the spectral traces depicted, all polypeptides display a broad centred minimum at 197 nm, which is characteristic of predominate random coil conformation (Fig. 3). A star homopolypeptide in the form of 64-PLL_{40} was analysed as a reference in order to compare the influence of the oligo(L-cysteine) block on the secondary structure. A large minimum (random coil) was observed for star PLL, indicative of the conformation noted due to interchain repulsion of cationic chains.[60] For the 32-arm core and shell copolypeptides, there is a moderate wavelength shift in the random coil minima, suggesting disparate disulphide crosslinking of the architectures via alternative β motifs. Although the slight increase from the disulphide β conformers is apparent, the individual characterisation of β turns and sheets are known to be difficult to determine from CD alone.[61] The position of the spontaneously formed cystine crosslinks on the periphery would contribute to a highly dense concentration of disulphides on the exterior of the hydrophilic poly-L-lysine segments, restricting the mobility of these inherently random coiling chains (Fig. 4).

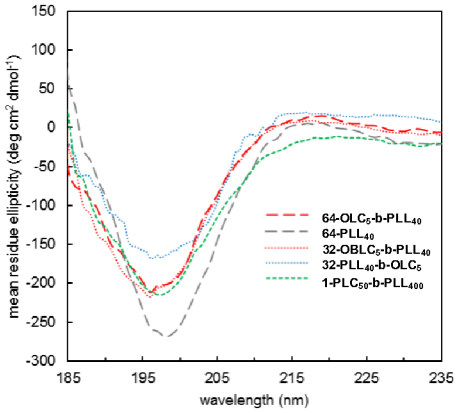

Fig. 3 CD (circular dichroism) spectra of copolypeptide samples in aqueous solution.

Polymer Chemistry

ARTICLE

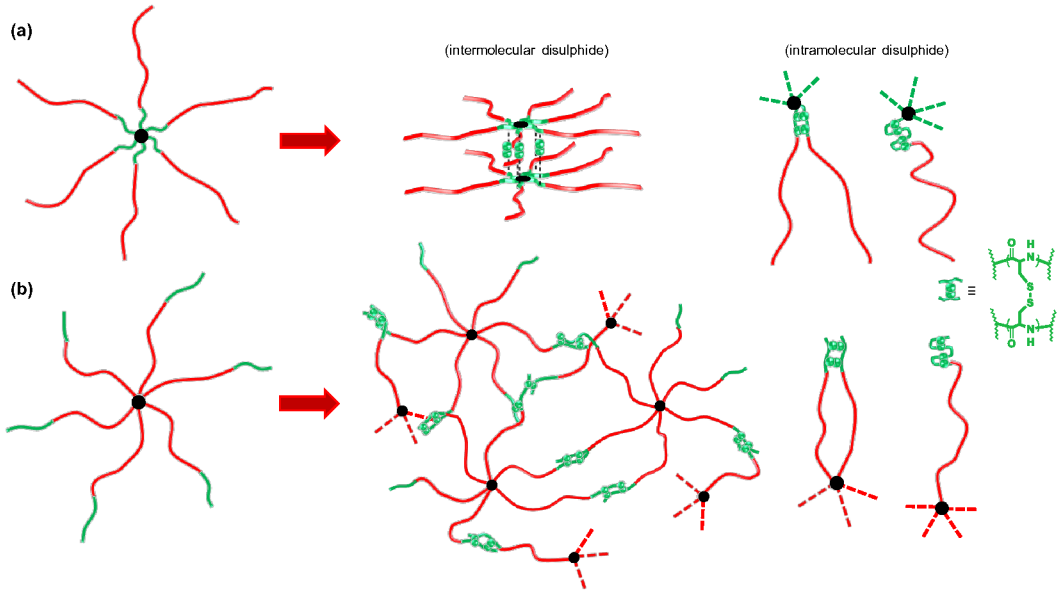

Fig. 4 Schematic representation of possible arrangements of core and shell disulphide crosslinked star copolypeptide hydrogels. (a) Star copolypeptide with OLC in the core. (b) Star copolypeptide with OLC on the shell.

While the core disulphide crosslinking would contribute to an inferior restriction of the shell PLL domains, allowing for an apparent increase in random coiling. Similarly, the CD spectral trace of 64-OLC_5-b-PLL_{40} did not deviate much from its 32-arm analogue, showing an almost identical intensity at the 197 nm minima. The inclusion of these alternate OLC blocks appears to reduce the degree of random coiling of PLL, which is known to undergo conformational shift in the presence of integrated assemblies.[62] The CD spectra of the linear block copolymer 1-PLC_{50}-b-PLL_{400}, with analogous composition, is in agreement with the prevailing disordered content. Although since the linear copolypeptide permits a mix of parallel and antiparallel assemblies, this could contribute to the evident broadening in the spectral region from 197-216 nm. Another interesting characteristic of the spectra, in addition to the minima mentioned, is the wide centred maxima at ~216 nm. Reports suggest such moderately intense maxima are indicative of the influence of β-motifs in a peptide-based architecture, signifying the impact of disulphide residues. These data suggest that indeed the majority of disulphide linkages occur through intermolecular interactions with the shell crosslinked hydrogel since the adjacent cysteine residues on the star architecture are ideally orientated for this. While the core oligo-L-cysteine containing hydrogel system appears to be mediated through primarily intramolecular interactions due to length and orientation of those sequences in the core. The highly ordered arrangement of β-turns or sheets from the alternative cysteine mediated assemblies provides core and shell diblock copolypeptide materials with different architecture and thus different spectral conformations.

Mechanical properties

The core and shell crosslinked star copolypeptides (32-OLC_5-b-PLL_{40} and 32-PLL_{40}-b-OLC_5) exhibited a distinctive linear visco-elastic (LVE) region in which storage modulus (G') exceeds the loss modulus (G''), see Fig. 5a. This is characteristic of materials that exhibit 'true gel'

behaviour. The position of the oligo(L-cysteine) sequence appears to afford different hydrogel mechanical properties as the recorded G' (in the LVE region) of the shell disulphide hydrogel was 4530 ± 8 Pa, which is far superior in strength to the core disulphide hydrogel, which has a G' of 820 ± 10 Pa. The length of the LVE region was different for the core and crosslinked copolypeptides hydrogels.

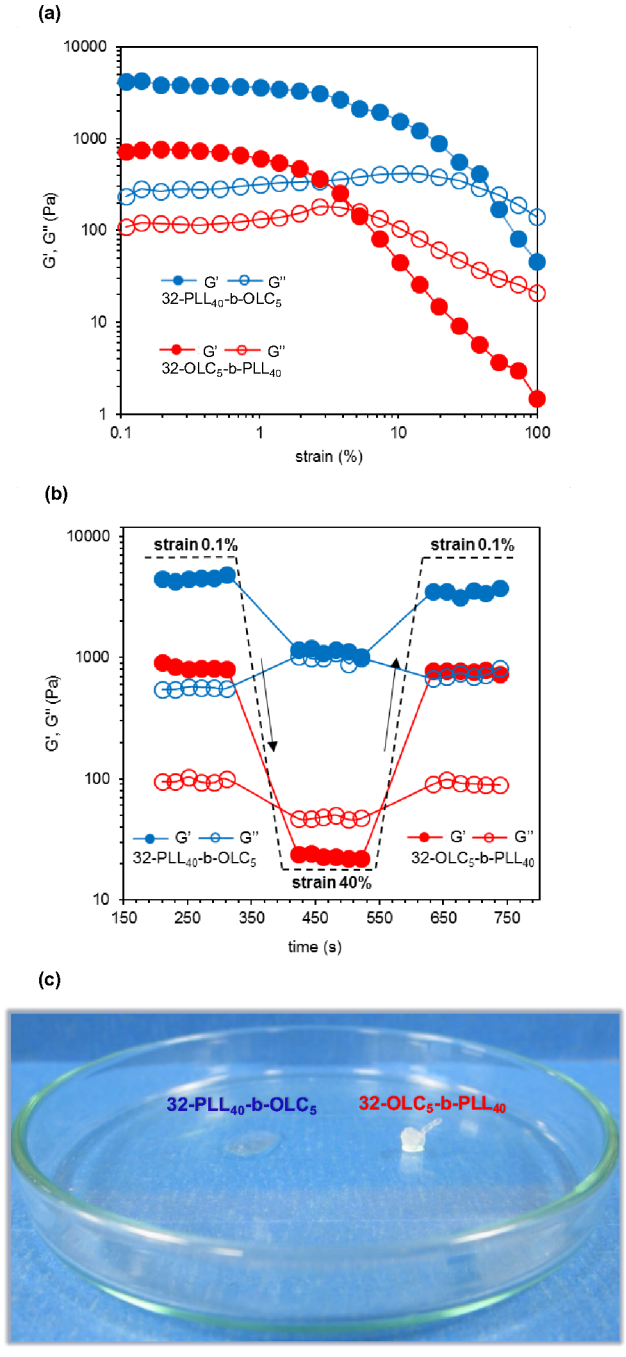

Fig. 5 Rheological (a) amplitude sweep of core and shell star copolypeptide hydrogels with storage and loss modulus as a function of increasing strain and constant frequency (sheared at $\dot{\gamma}$ = 0.1–100, ω = 1 rad s^{-1}). Rheological (b) short stepping strain sweep of core and shell disulphide crosslinked star copolypeptides (at constant frequency ω = 1 rad s^{-1}). (c) Image of both hydrogels after shearing through a standard 21G syringe needle (video ESI).

For example, the *G'* value of 32-PLL_{40}-b-OLC_5 decreased upon reaching 2% (indicating the end of the LVE region) and had a crossover point with *G''* at 48%. This is representative of a gel-sol transition, flow behaviour. In comparison, the crossover point was at 5% strain for the shell crosslinked 32-OLC_5-b-PLL_{40} hydrogel. The hydrogels' self-recovery behaviour was investigated through a short step strain sweep experiment (Fig. 5b). The use of 40% strain was insufficient to induce a gel-sol transition of 32-PLL_{40}-b-OLC_5 as G'' did not exceed G'. Although, the large amplitude strain did have an effect on the self-recovery behaviour of the hydrogel network. The initial G' of 32-OLC_5-b-PLL_{40} was 811 ± 15 Pa, which reverted to 782 ± 12 Pa after the strain cycling, corresponding to full self-recovery (within error margins). In contrast, the hydrogel formed for 32-PLL_{40}-b-OLC_5 exhibited a self-recovery of about 75%, i.e. initial G' value of 4521 ± 9 Pa, which recovered to 3515 ± 11 Pa after returning to original strain. The results demonstrate that the position of the disulphide crosslinks within these star copolypeptide hydrogels can impart two distinctively different mechanical behaviours otherwise unattainable in linear polypeptide analogues. The practical aspect of this was demonstrated by assessing the ability to inject these hydrogels through a standard 21G syringe needle (Fig. 5c). The core crosslinked hydrogel underwent shear deformation reforming almost instantaneously after passing through the needle while the shell crosslinked hydrogel expelled water when subject to the same shear (video, ESI), further substantiating the rheological analysis. For the 32-arm and 64-arm core crosslinked hydrogels, there is a direct correlation between relative strength of the gel and increasing degree of branching (G' values of 820 ± 10 Pa and 1230 ± 13 Pa, respectively).

In comparison to its 32-arm counterpart, the 64-arm hydrogel sample showed network breakdown (end of LVE region) at >5% strain (Fig. S5a) while both hydrogels were insensitive to frequency fluctuation (Fig. S5b). A step strain sweep experiment (Fig. S5c)

demonstrated the self-recovery behaviour of the core crosslinked hydrogels. Above the significant amplitude oscillatory strain (40%), expected deformation was evident as G' sharply reduced. Reverting back to 0.1% strain which was within the viscoelastic threshold allowed for recovery of G' to its original value. Even after stepping the strain to a higher amplitude (60%), the G' of both star copolypeptides promptly returned to their original state upon a return to 0.1% strain (indicating self-recovery behaviour).

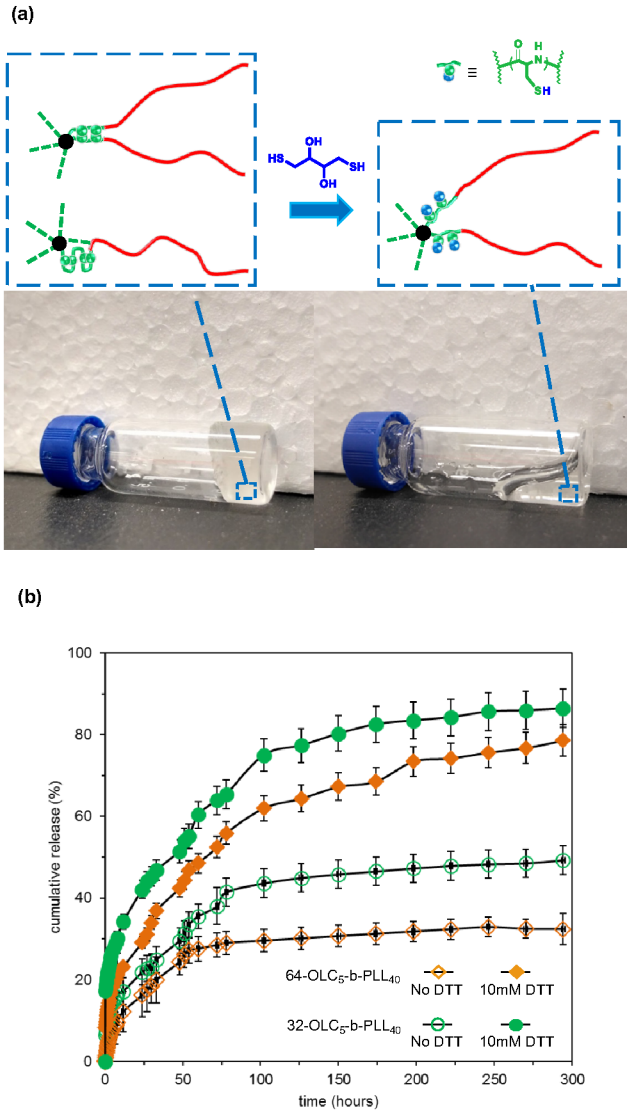

Fig. 6 (a) 64-OLC_5-b-PLL_{40} hydrogel and reduction of 64-OLC_5-b-PLL_{40} hydrogel using 10mM DTT. (b) Cumulative DOX release from DOX-loaded star copolypeptide hydrogels over 12-day period in presence and absence of 10 mM DTT.

Drug release

Since the core crosslinked hydrogels exhibit favourable rheological behaviour in terms of shear-thinning, they were further examined for their drug release properties (Fig. 6), based on their potential as injectable or 3D printable matrices for therapeutic delivery. DOX.HCl was loaded into each of the star block copolypeptide hydrogels (32- and 64-arm) by vigorously mixing the lyophilised samples with the DOC.HCl solution (1 mg mL^{-1}) at room temperature at a polypeptide concentration of 3.0 wt%. In order to illustrate the redox response of the disulphide linkages, two different concentrations of DTT were added to the hydrogels (5 mM and 10 mM). Almost instantly, the homogeneity of the hydrogels became unstable resulting in material flow (Fig. 6a). The release profile of DOX from the star shaped hydrogels was examined in the absence and presence of DTT, in order to simulate both a redox free and redox environment (Fig. 6b). The release of DOX for all samples eventually plateaued after the 300 hours (~12 day) of the study. Cumulative release of DOX reached 32% and 49% for the 64-arm and 32-arm block copolypeptide hydrogels respectively over 12 days. Interesting to note is the correlation between the release profile and the degree of branching. The 64-arm hydrogel depot had a more delayed release of DOX which is most likely due to the increasing degree of branching of the star architecture in addition to the attached polypeptide arms, meaning simultaneous degradation and diffusion would be slower. Therefore, the closely aligned core would more readily envelop the loaded drug thus prolonging the release. DTT accelerated the release of DOX from both platforms via cleavage of the core disulphide bonds prompting destruction of the hydrogel network and thus diffusion through the corona of the star polypeptide.

After a period of 100 hours (~4 days), and in the absence of DTT, the sample 64-OLC_5-b-PLL_{40} released 29% of its cargo while in comparison 61% of DOX was released when the hydrogels were exposed to DTT. The hydrogels incubated with PBS without DTT present still triggered release without any prior stimulation from a reductant, implying that the dendrimer core of the molecule did not encapsulate a significant amount of the payload. This could be a result of the covalent crosslinks within the star copolypeptide. The density of disulphide residues on the edge in the inner core would promote slow diffusion of DOX into the PPI dendritic core, meaning the drug payload would localise at the periphery of the core.

Conclusions

A series of star shaped diblock copolypeptides containing core and shell disulphide crosslinks were synthesised by alternating oligo-L-cysteine and poly-L-lysine sequences. In aqueous solution, the star copolypeptides formed stable hydrogels with material content as low as polymer 0.05 wt%. Changing the sequence on the 32-arm PPI dendrimer from core crosslinking to shell crosslinking had a significant effect on hydrogel storage modulus as it changed from 820 ± 10 Pa to 4530 ± 8 Pa. Moreover, the core crosslinked hydrogel underwent self-recovery almost instantaneously after passing through a standard syringe needle while the shell crosslinked hydrogel expelled water when subject to the same shear. Hydrogels readily underwent network disruption after the addition the molecular reductant DTT, cleaving disulphide bonds resulting in a gel-sol transition, which was utilised to accelerate the release of the model drug doxorubicin from the hydrogel depots. The diverse material properties associated with the star copolypeptide system employed here allows for fabrication of stable hydrogels bearing high mechanical strength or shear thinning properties by simply adjusting the sequence order, while simultaneously possessing redox responsiveness. The rheological behaviour of these core crosslinked copolypeptides coupled with their innate redox responsiveness makes them ideal for applications that require shear-thinning redox sensitive materials such as cardiac tissue engineering.

Conflicts of Interest

There are no conflicts of interest to declare

Acknowledgements

Financial support from a Science Foundation Ireland (SFI) Principle Investigator Award 13/IA/1840(T) is gratefully acknowledged. MihP would like to thank Australian Research Council Centres of Excellence Program (CE140100012) and University of Wollongong for financial assistance.

References

[1] D. Seliktar, *Science* 2012, **336**, 1124–1128.
[2] O. Jeon, K. H. Bouhadir, J. M. Mansour and E. Alsberg, *Biomaterials*, 2009, **30**, 2724–2734.
[3] J. T. Zhang, R. Bhat and K. D. Jandt, *Acta Biomaterialia*, 2009, **5**, 488–497.
[4] M. Nakahata, Y. Takashima, H. Yamaguchi and A. Harada, *Nat. Commun*., 2011, **2**, 511–516.
[5] A. B. South and L. A. Lyon, *Angew. Chem*., 2010, **122**, 779–783.
[6] M. Guvendiren, H. D. Lu, and J. A. Burdick, *Soft Matter*, 2012, **8**, 260–272.
[7] S. Zhang, M. Altman, *React. Funct. Polym*., 1999, **41**, 91–102.
[8] B. S. Berlett and E. R. Stadtman, *J. Biol. Chem*., 1997, **272**, 20313–20316.
[9] L. E. R. O'Leary, J. A. Fallas, E. L. Bakota, M. K. Kang and J. D. Hartgerink, *Nat. Chem*., 2011, **3**, 821–828.
[10] L. D. D'Andrea, and L. Regan, *Trends Biochem. Sci*., 2003, **28**, 655–662.
[11] P. T. Lansbury Jr, P. R. Costa, J. M. Griffiths, E. J. Simon, M. Auger, K. J. Halverson, D. A. Kocisk, Z. S. Hendsch, T. T. Ashburn, R. G. S. Spencer, B. Tidor and R. G. Griffin, *Nature Struct. Biol*., 1995, **2**, 990–998.
[12] R. Fairman and K. S. Akerfeldt, *Curr. Opin. Struct. Biol*., 2005, **15**, 453–463.
[13] S. J. Shirbin, F. Karimi, N. J. A. Chan, D. E. Heath and G. G.Qiao, *Biomacromolecules*, 2016, **17**, 2981–2991.
[14] C. C. Ahrens, M. E. Welch, L. G. Griffith and P. T. Hammond, *Biomacromolecules*, 2015, **16**, 3774–3783.
[15] H. Cui, X. Zhuang, C. He, Y. Wei and X. Chen, *Acta Biomater*., 2015, **11**, 183–190.
[16] T. Stukenkemper, J. F. G. A. Jansen, C. Lavilla, A. A. Dias, D. F. Brougham and A. Heise, *Polym. Chem*., 2017, **8**, 828–832.
[17] T. Borase and A. Heise, *Adv. Mater*., 2016, **28**, 5725–5731.
[18] J. Yuan, Y. Sun, J. Wang, H. Lu, *Biomacromolecules,* 2016, **17**, 891–896.
[19] Deming, T. J. Synthesis of Side-Chain Modified Polypeptides. *Chem. Rev.,* **2015**, *116*, 786-808.
[20] K. Ren, C. He, C. Xiao, G. Li and X. Chen, *Biomaterials*, 2015, **51**, 238–249.
[21] L. Yin, Z. Song, K. H. Kim, N. Zheng, H. Tang, H. Lu, N. Gabrielson and J. Cheng, *Biomaterials*, 2013, **34**, 2340–2349.
[22] A. P. Nowak, V. Breedveld, L. Pakstls, B. Ozbas, D. J. Plne, D. Pochan and T. J. Deming, *Nature* **2002**, *417*, 424-428.
[23] E. F. Banwell, E. S. Abelardo, D. J. Adams, M. A. Birchall, A. Corrigan, A. M. Donald, M. Kirkland, L. C. Serpell, M. F. Butler and D. N. Woolfson, *Nat. Mater*., 2009, **8**, 596–600.
[24] M. C. Giano, D. J. Pochan and J. P. Schneider, *Biomaterials,* 2011, **32**, 6471–6477.
[25] C. Zhao, X. Zhuang, P. He, C. Xiao, C. He, J. Sun, X. Chen and X. Jing, *Polymer*, 2009, **50**, 4308–4316.
[26] S. Zhang, D. J. Alvarez, M. V. Sofroniew and T. J. Deming, *Biomacromolecules*, 2015, **16**, 1331–1340.
[27] J. Huang, C. L. Hastings, G. P. Duffy, H. M. Kelly, J. Raeburn, D. J. Adams and A. Heise, *Biomacromolecules*, 2013, **14**, 200–206.
[28] M. Zhu, Y. Wu, C. Ge, Y. Ling, and H. Tang, *Macromolecules*, 2016, **49**, 3542–3549.
[29] J. R. Kramer and T. J. Deming, *J. Am. Chem. Soc.*, 2012, **134**, 4112–4115.
[30] G. E. Negri and T. J. Deming, *ACS Macro Letters* 2016, **5,** 1253-1256.
[31] G. Liu and C. M. Dong, *Biomacromolecules*, 2012, **13**, 1573–1583.
[32] M. L. Circu and T. Y. Aw, *Free Radic. Res*., 2008, **42**, 689–706.

[33] E. P. Feener, W.C. Shen and H. J. P. Ryser, *J. Biol. Chem.*, 1990, **265**, 18780–18785.
[34] H. F. Gilbert, *Methods Enzymol*. 1995, **251**, 8–28.
[35] D. Wu, X. J. Loh, Y.-L. Wu, C. L. Lay and Y. Liu, *J. Am. Chem. Soc.*, 2010, **132**, 15140–15143.
[36] X. Wang, D. Li, F. Yang, H. Shen, Z. Li and D. Wu, *Polym. Chem.*, 2013, **4**, 4596−4600.
[37] B. S. McAvan, M. Khuphe and P. D. Thornton, *Eur. Polym. J.*, 2017, **87**, 468–477.
[38] Y. X. Zhang, Y.-F.; Chen, X.-Y. Shen, J.-J. Hu and J.-S. Jan, *Polymer* 2016, **86**, 32–41.
[39] J. Zhou, P. Chen, C. Deng, F. Meng, R. Cheng and Z. Zhong, *Macromolecules*, 2013, **46**, 6723−6730.
[40] T. Xing, C. Mao, B. Lai and L. Yan, *ACS Appl. Mater. Interfaces*, 2012, **4**, 5662−5672.
[41] Y. Ma, X. Fu, Y. Shen, W. Fu and Z. Li, *Macromolecules*, 2014, **47**, 4684–4689.
[42] S. Zhang, Y. Wan, W. Fu and Z. Li, *Soft Matter*, 2015, **15**, 2945–2951.
[43] P. D. Thornton, S. M. R. Billah and N. R. Cameron, *Macromol. Rapid Commun.*, 2013, **34**, 257–262.
[44] R. Murphy, T. Borase, C. Payne, J. O'Dwyer, S. A. Cryan and A. Heise, *RSC Adv.*, 2016, **6**, 23370–23376.
[45] R. Murphy, D. P. Walsh, C. A. Hamilton, S. A. Cryan, M. in het Panhuis and A. Heise, *Biomacromolecules*, 2018, DOI: 10.1021/acs.biomac.8b00299.
[46] D. L. Liu, X. Chang and C. M. Dong, *Chem. Commun.*, 2013, **49**, 1229–1231.
[47] M. Byrne, D. Victory, A. Hibbitts, M. Lanigan, A. Heise and S. A. Cryan, *Biomater. Sci.*, 2013, **1**, 1223–1234.
[48] M. Byrne, P. D. Thornton, S. A. Cryan, and A. Heise, *Polym. Chem.*, 2012, **3**, 2825–2831.
[49] C. Lavilla, M. Byrne and A. Heise, *Macromolecules* 2016, **49**, 2942−2947.
[50] C. Lavilla, G. Yilmaz, V. Uzunova, R. Napier, C. R. Becer and A. Heise, *Biomacromolecules* 2017, **18**, 1928−1936.
[51] P. D. Walsh, R. Murphy, A. Panarella, R.M. Raftery, B. Cavanagh, J. Simpson, F. J. O'Brien, A. Heise and S.-A. Cryan, *Mol. Pharmaceutics* 2018, DOI: 10.1021/acs.molpharmaceut.8b00044.
[52] A. Sulistio, A. Widjaya, A. Blencowe, X. Zhang and G. G. Qiao, *Chem. Commun.*, 2011, **47**, 1151−1153.
[53] Q. Chen, F. Han, C. Lin, X. Wen and P. Zhao, *Polymer*, 2018, **146**, 378−385.
[54] S.-S. Cheng, K. K. Chittur, C. N. Sukenik, L. A. Culp and K. J. Lewandowska, *J. Colloid Interface Sci.*, 1994, **162**, 135−143.
[55] A. Ravi and P. Balaram, *Tetrahedron*, 1984, **40**, 2577−2583.
[56] V. Moretto, M. Crisma, G. M. Bonora and C.Toniolo, *Macromolecules*, 1989, **22**, 2939−2944.
[57] M. Hollosi, Z. Majer, A. Z. Ronai, A. Magyar, K. Medzihradszky, S. Holly, A. Perczel, and G. D. Fasman, Biopolymers, 1994, **34**, 177−185.
[58] T. J. Cashman and B. R. Linton, *Org. Lett.*, 2007, **9**, 5457-5460
[59] R. Kishore, S. Raghothama, and P. Balaram, 1987, *Biopolymers*, **26**, 873−891.
[60] J. S. Chiou, T. Tatara, S. Sawamura, Y. Kaminoh, H. Kamaya, A. Shibata and I. Ueda, *Biochim. Biophys. Acta.*, 1992, **1119**, 211–217.
[61] A. Glattli, X. Daura, D. Seebach and W. F. van Gunsteren, *J. Am. Chem. Soc.*, 2002, **124**, 12972– 12978.
[62] A. Harada, S. Cammas and K. Kataoka, Macromolecules, 1996, **29**, 6183–6188.

ToC

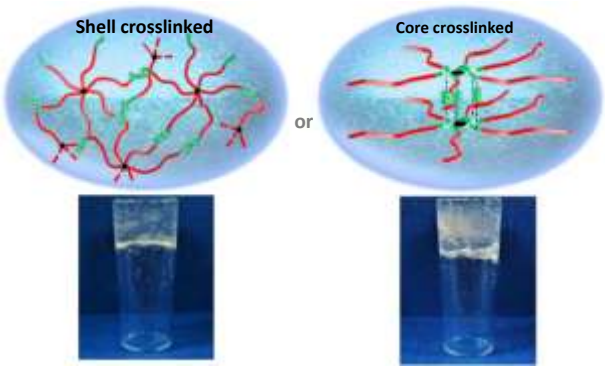

Strong redox responsive hydrogels with mechanical properties depending on the positioning of oligo(cysteine) within the star polypeptides were obtained.